

# AIMP2/p38, the scaffold for the multi-tRNA synthetase complex, responds to genotoxic stresses via p53

Jung Min Han\*, Bum-Joon Park\*, Sang Gyu Park\*, Young Sun Oh\*, So Jung Choi\*, Sang Won Lee\*, Soon-Kyung Hwang<sup>†</sup>, Seung-Hee Chang<sup>†</sup>, Myung-Haing Cho<sup>†</sup>, and Sunghoon Kim\*\*

\*Center for Medicinal Protein Network and Systems Biology, College of Pharmacy, and <sup>†</sup>College of Veterinary Medicine, Seoul National University, Seoul 151-742, Korea

Edited by Moshe Oren, Weizmann Institute of Science, Rehovot, Israel, and accepted May 5, 2008 (received for review January 10, 2008)

**AIMP2/p38 is a scaffolding protein required for the assembly of the macromolecular tRNA synthetase complex. Here, we describe a previously unknown function for AIMP2 as a positive regulator of p53 in response to genotoxic stresses. Depletion of AIMP2 increased resistance to DNA damage-induced apoptosis, and introduction of AIMP2 into AIMP2-deficient cells restored the susceptibility to apoptosis. Upon DNA damage, AIMP2 was phosphorylated, dissociated from the multi-tRNA synthetase complex, and translocated into the nuclei of cells. AIMP2 directly interacts with p53, thereby preventing MDM2-mediated ubiquitination and degradation of p53. Mutations in AIMP2, affecting its interaction with p53, hampered its ability to activate p53. Nutlin-3 recovered the level of p53 and the susceptibility to UV-induced cell death in AIMP2-deficient cells. This work demonstrates that AIMP2, a component of the translational machinery, functions as proapoptotic factor via p53 in response to DNA damage.**

aminoacyl-tRNA synthetase | JNK | apoptosis | DNA damage | mdm2

**A**minoacyl-tRNA synthetases (ARSs) are the enzymes that ligate specific amino acids to tRNAs before protein synthesis. In higher eukaryotic systems, nine different ARSs form an intriguing macromolecular complex with three nonenzymatic factors called ARS-interacting, multifunctional proteins (AIMPs) (1, 2). Many of these complex-forming ARSs, as well as AIMPs, play diverse regulatory roles that are not directly related to protein synthesis (2). Among the three AIMPs, AIMP1 is secreted as a cytokine working in immune, angiogenesis, and wound-healing processes (3–7) and also functions as a hormone controlling glucose homeostasis (8). AIMP3 is a tumor suppressor required for chromosome integrity (9, 10). Although AIMP2 is critical for the assembly of the multi-ARS complex (11), it also suppresses cell proliferation via down-regulation of c-Myc (12). In addition, AIMP2 was shown to be involved in Parkinson's disease, inducing neural cell death (13). However, it is yet to be determined how AIMP2 is involved in the control of cell death. In this work, we investigated the functional significance and molecular behavior of AIMP2 during the control of cell death and the relationship of AIMP2 associated with the multi-ARS complex and its proapoptotic activity.

## Results

**AIMP2-Deficient Cells Are Resistant to Cell Death.** To see the importance of AIMP2 during the control of cell death, we subjected 12.5-d *AIMP2*<sup>+/+</sup> and *AIMP2*<sup>-/-</sup> mouse embryonic fibroblasts (MEFs) to UV irradiation and compared their apoptotic sensitivity. The apoptotic cells, indicated by the subG1 portion, were increased ≈3-fold by UV irradiation in *AIMP2*<sup>+/+</sup> but not in *AIMP2*<sup>-/-</sup> cells (Fig. 1A). Transfection of *AIMP2* into *AIMP2*<sup>-/-</sup> MEFs restored the apoptotic sensitivity to UV irradiation (Fig. 1B). We also compared the apoptotic response of *AIMP2*<sup>+/+</sup> and *AIMP2*<sup>-/-</sup> MEFs to UV irradiation by monitoring caspase-3 activation. Procaspase-3 cleavage resulting in caspase-3 generation was observed

in *AIMP2*<sup>+/+</sup> but not in *AIMP2*<sup>-/-</sup> cells (Fig. 1C). Suppression of AIMP2 via gene-specific siRNA (14) also rendered the cells resistant to UV-induced cell death as determined by annexin V- and PI-positive populations by using flow cytometry (Fig. 1D). When thymocytes isolated from *AIMP2*<sup>+/+</sup> and *AIMP2*<sup>+/-</sup> mice were compared for their apoptotic response to adriamycin-induced DNA damage, *AIMP2*<sup>+/-</sup> cells showed a higher resistance to apoptosis [supporting information (SI) Fig. S1]. Thymocytes could not be obtained from *AIMP2*<sup>-/-</sup> mice because of their neonatal lethality (11, 12). Conversely, overexpression of AIMP2 enhanced UV-induced cell death (Fig. 1E), suggesting a proapoptotic function for AIMP2.

**DNA Damage Induces Phosphorylation and Dissociation of AIMP2 from the Multi-ARS Complex, as Well as Its Nuclear Translocation.** Next, we monitored the molecular behavior of AIMP2 under genotoxic stress to understand the proapoptotic activity of AIMP2. Although the main portion of AIMP2 was detected in the cytosol, its nuclear portion was increased 3–10 min after UV irradiation (Fig. 2A). To see whether nuclear accumulation of AIMP2 involves its *de novo* synthesis, we transfected *Myc-AIMP2*, blocked protein synthesis with cycloheximide (CHX), and then subjected the cells to UV irradiation. The nuclear localization of *Myc-AIMP2* increased along with a slight decrease in the cytosolic portion 10 min after UV irradiation (Fig. S2), suggesting that the increase in the nuclear portion did not involve new synthesis of AIMP2 during this time period.

Considering that the increase in nuclear AIMP2 does not require *de novo* synthesis, AIMP2 bound to the multi-ARS complex is the likely source for this nuclear portion. We thus investigated whether AIMP2 is posttranslationally modified upon UV irradiation. AIMP2 extracted from the control and UV-irradiated cells were separated by 2D gel electrophoresis. Although AIMP2 of the control cells was detected mainly as a single spot, a few additional spots were generated in the more acidic region upon UV irradiation and disappeared after treatment with alkaline phosphatase (AP) (Fig. 2B), indicating that AIMP2 is phosphorylated after UV irradiation. Proteins were extracted from the UV-irradiated cells, immunoprecipitated with an anti-AIMP2 antibody, and blotted with anti-p-Ser, -Thr, and -Tyr antibodies. It was observed that

Author contributions: J.M.H., M.-H.C., and S.K. designed research; J.M.H., B.-J.P., S.G.P., Y.S.O., S.J.C., S.W.L., S.-K.H., and S.-H.C. performed research; S.-K.H., S.-H.C., and M.-H.C. contributed new reagents/analytic tools; J.M.H. analyzed data; and J.M.H. and S.K. wrote the paper.

The authors declare no conflict of interest.

This article is a PNAS Direct Submission. M.O. is a guest editor invited by the Editorial Board.

\*To whom correspondence should be addressed. E-mail: sungkim@snu.ac.kr.

This article contains supporting information online at [www.pnas.org/cgi/content/full/0800297105/DCSupplemental](http://www.pnas.org/cgi/content/full/0800297105/DCSupplemental).

© 2008 by The National Academy of Sciences of the USA

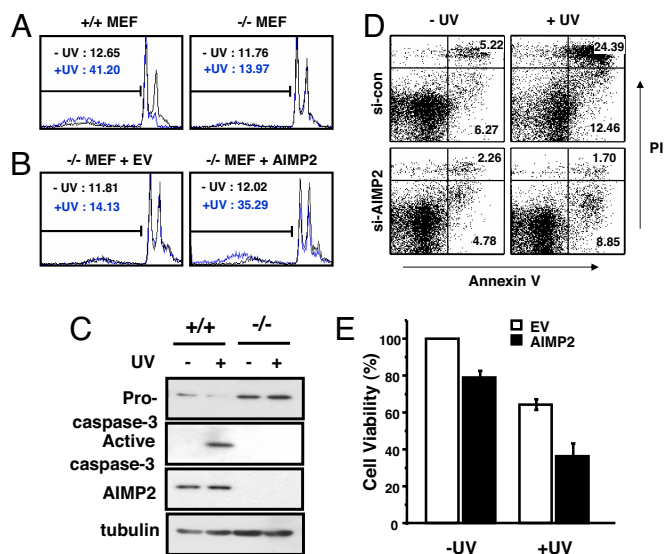


**Fig. 1.** AIMP2 is critical for the control of cell death. (A) *AIMP2*<sup>+/+</sup> and *AIMP2*<sup>-/-</sup> MEFs were irradiated by UV (50 J/m<sup>2</sup>) and measured for the presence of apoptotic cells by flow cytometry after 6 h. The bars and numbers indicate the subG1 phase cells and their percentages, respectively. (B) After transfection of *AIMP2* or empty vector (EV) into *AIMP2*<sup>-/-</sup> MEFs for 24 h, the cells were treated with UV, and the subG1 phase cells were measured as above. (C) *AIMP2*<sup>+/+</sup> and *AIMP2*<sup>-/-</sup> MEFs were subjected to UV irradiation as above, and after 3 h, the generation of active caspase-3 from pro-caspase-3 was monitored by Western blotting with anti-pro-caspase-3, -active caspase-3, -AIMP2, and tubulin antibodies. (D) The effect of AIMP2 suppression with AIMP2 siRNA on UV-induced U2OS cell death was monitored by flow cytometry using FITC-annexin V and PI. Viable, early apoptotic, and late apoptotic cells are FITC<sup>-</sup> PI<sup>-</sup>, FITC<sup>+</sup> PI<sup>-</sup>, and FITC<sup>+</sup> PI<sup>+</sup>, respectively. The numbers represent percentages of the corresponding cells. (E) U2OS cells were transfected with EV or AIMP2 and treated with UV (50 J/m<sup>2</sup>). After 12 h, the effect of AIMP2 on UV-induced cell death was measured by colorimetric thiazoyl blue assay. The bars represent the mean ± SD, from triplicate samples.

AIMP2 specifically reacted with an anti-*p*-Ser antibody, indicating its phosphorylation at serine residue(s) (Fig. 2C).

To see whether UV irradiation would induce the dissociation of AIMP2 from the multi-ARS complex, proteins were extracted from the control and UV-irradiated cells and then fractionated by gel filtration. Whereas the components bound to the multi-ARS complex would be coeluted in the void volume, those dissociated from the complex are expected to be eluted in the later fractions (14). Although AIMP2 was coeluted with the largest enzyme component of the complex, glutamyl-prolyl-tRNA synthetase (EPRS), in the control cells (Fig. 2D Upper), it was detected in two different fractions in the UV-treated cells, one in the void volume with EPRS and the other in the later fractions (Fig. 2D Lower). This suggested that UV irradiation induced the dissociation of AIMP2 from the complex. We then compared AIMP2 obtained from the two fractions (fractions 24 and 36) by 2D gel electrophoresis. Although AIMP2 in the void volume resolved at the same position in the 2D gel as that of the control cells, AIMP2 in the later fraction was detected at the location of phosphorylated AIMP2 (Fig. 2E). To see whether phosphorylated AIMP2 is located in the nucleus, the UV-irradiated cells were separated into cytosol and nuclear fractions, and AIMP2 was analyzed by 2D gel electrophoresis as above. The nuclear AIMP2 fraction was shifted into the acidic region relative to the cytosolic form and was returned to its original position by treatment with AP (Fig. 2F), indicating that nuclear AIMP2 is phosphorylated.

To gain insight into the putative kinase(s) involved in the phosphorylation of AIMP2, we treated the cells with inhibitors against different kinases such as casein kinase II (15), protein kinase

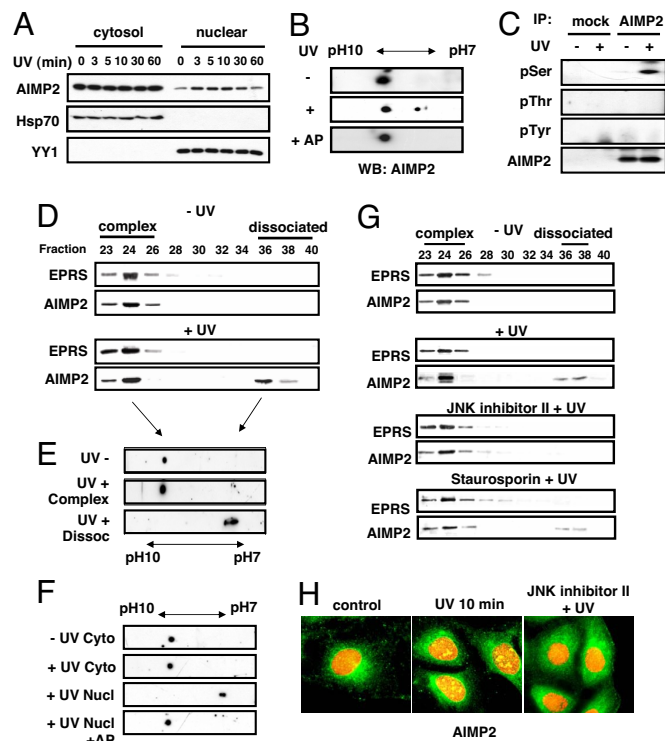


**Fig. 2.** UV-dependent phosphorylation, complex dissociation, and nuclear localization of AIMP2. (A) U2OS cells were UV irradiated (50 J/m<sup>2</sup>), and the cytoplasmic and nuclear fractions were separated by using a subcellular proteome extraction kit (Calbiochem). The proteins extracted from each fraction were immunoblotted with the antibodies against AIMP2, YY1 (nuclear marker), and Hsp70 (cytoplasmic marker). (B) U2OS cells were UV irradiated (50 J/m<sup>2</sup>). After 5 min, cells were harvested and proteins extracted from the untreated (Top) and UV-treated cells (Middle) were separated by 2D gel electrophoresis and subjected to Western blotting with an anti-AIMP2 antibody. To determine the UV-dependent phosphorylation of AIMP2, the proteins extracted from the UV-treated cells were reacted with +AP (Bottom). (C) Lysates from U2OS cells, irradiated with UV for 5 min, were immunoprecipitated with anti-AIMP2 antibody and immunoblotted against pSer, pThr, pTyr. (D) To determine the effect of UV irradiation on the dissociation of AIMP2, the proteins prepared as above were separated by gel filtration, and the eluted fractions from 23 to 40 were subjected to SDS/PAGE. AIMP2 and EPRS were detected by Western blotting with their respective antibodies. (E) The proteins in fractions 24 and 36 were precipitated with a 2D clean-up kit (GE Healthcare) and then subjected to 2D gel electrophoresis and Western blotting with anti-AIMP2 antibody. (F) U2OS cells were UV irradiated, harvested at 5 min, and the cytoplasmic and nuclear fractions were separated by using a subcellular proteome extraction kit (Calbiochem). The proteins extracted from both fractions were precipitated with a 2D clean-up kit (GE Healthcare), treated with AP, and then subjected to 2D gel electrophoresis. The migration of AIMP2 was determined by immunoblotting with an anti-AIMP2 antibody. (G) U2OS cell, treated or untreated with JNK inhibitor II (20 μM) or staurosporin (0.5 μM), were UV irradiated. The proteins extracted from the cells were subjected to gel filtration, SDS/PAGE, and Western blot analysis for EPRS and AIMP2 as above. (H) U2OS cells (control, 10 min after UV, 10 min after UV, and JNK inhibitor II treated) were stained with anti-AIMP2 antibody (green) and counterstained with PI (red) to monitor the cellular localization of AIMP2. Data are representative of three independent experiments.

C (16), and Jun N-terminal kinase (17) that are known to respond to UV irradiation and checked the phosphorylation of AIMP2. The phosphorylation of AIMP2 was specifically inhibited by JNK inhibitor II (Fig. S3A), implying that JNK is a potential upstream kinase responsible for the phosphorylation of AIMP2. However, further analysis is needed to determine whether JNK works directly

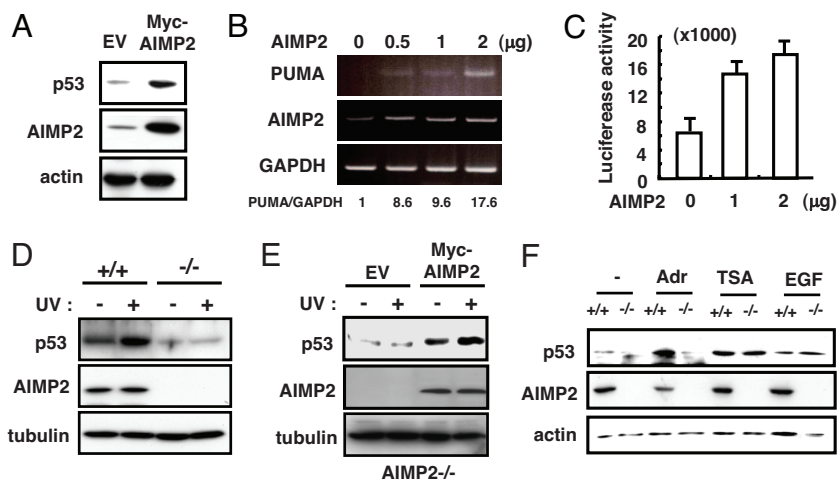


**Fig. 3.** Functional significance of AIMP2 activation of p53 in response to DNA damage. (A) The effect of AIMP2 on p53 levels was monitored by using Western blotting after transfection of AIMP2 into U2OS cells that were p14<sup>Arf</sup> inactive, to exclude the possible involvement of p14<sup>Arf</sup> in the induction of p53. (B) AIMP2 was transfected into U2OS cells at the indicated amounts and its effect on the expression of p53, further supported by the expression of PUMA, a known target of p53, was monitored by RT-PCR. GAPDH was used as the control. (C) After cotransfection with the indicated amounts of AIMP2 and *GADD45-luciferase* (0.5 µg/ml), U2OS cells were incubated for 24 h and dissolved in lysis buffer (Promega). After collection by centrifugation, cells were lysed, mixed with the luciferase reaction substrate, and the reaction was quantified by using a luminometer. (D) *AIMP2*<sup>+/+</sup> and *AIMP2*<sup>-/-</sup> MEFs were irradiated by UV at 50 J/m<sup>2</sup> and the extracted proteins were subjected to immunoblotting with anti-p53, -AIMP2, and -tubulin antibodies. (E) AIMP2-deficient MEFs were transfected with EV or AIMP2. They were then treated with UV and checked whether p53 activation was restored by the exogenous introduction of AIMP2. (F) To determine whether AIMP2 is specifically required for the activation of p53, we treated *AIMP2*<sup>+/+</sup> and *AIMP2*<sup>-/-</sup> MEFs with adriamycin (1 µg/ml, 4 h), TSA (100 ng/ml, 12 h), and EGF (10 ng/ml, 4 h), then compared the cellular levels of p53 by Western blotting. Actin was used as a loading control. Data are representative of three independent experiments.

on AIMP2. Because JNK is one of the MAPKs, we also checked whether the two other known MAPKs, ERK and p38 MAPK, are also involved in the phosphorylation of AIMP2 by using the inhibitors U0126 and SB202190, respectively. These inhibitors did not affect the UV-induced phosphorylation of AIMP2 (Fig. S3B), further supporting the specific involvement of JNK in the phosphorylation of AIMP2. To see whether the phosphorylation of AIMP2 is necessary for its dissociation from the multi-ARS complex and nuclear translocation, we treated the cells with JNK inhibitor II. Although the dissociated form of AIMP2 was detected in UV-irradiated cells, its generation was blocked by the treatment with JNK inhibitor II but not by staurosporin (Fig. 2G). JNK inhibitor II also blocked the nuclear localization of AIMP2 (Fig. 2H). These results suggest that JNK-dependent phosphorylation of AIMP2 is required for the dissociation of AIMP2 from the multi-ARS complex and its nuclear localization.

**AIMP2 Controls the p53 Response to DNA Damage.** Because p53 plays a critical role in the apoptotic response to DNA damage, we checked whether the function of AIMP2 during apoptosis would involve the p53 pathway. The proapoptotic activity of AIMP2 was ablated when p53 was suppressed via siRNA in U2OS cells (Fig. S4), suggesting a functional linkage between p53 and AIMP2. We then analyzed whether AIMP2 would regulate p53. Transfection of AIMP2 increased p53 levels (Fig. 3A) as well as the expression of p53-up-regulated modulator of apoptosis (PUMA), a known target of p53 (Fig. 3B). It also increased the expression of a reporter gene controlled by the p53-dependent *GADD45* promoter (Fig. 3C) in a dose-dependent manner. The p53 levels and the response to UV irradiation were significantly suppressed in *AIMP2*<sup>-/-</sup> cells (Fig. 3D), but p53 cellular levels were enhanced when AIMP2 was introduced into *AIMP2*<sup>-/-</sup> MEFs (Fig. 3E). Immunofluorescence staining and Western blot analysis of p53 also showed that UV- or adriamycin-dependent induction of p53 was abolished when AIMP2 was suppressed with AIMP2 siRNA (Fig. S5A and B).

To determine the functional specificity of AIMP2 during the control of cell death, we treated the cells with the histone deacetylase inhibitor, trichostatin A (18, 19), and mitogenic epidermal

growth factor (EGF) (20), which are known to activate p53, in addition to adriamycin. All of these treatments increased p53 levels in WT MEFs (Fig. 3F) or nonspecific siRNA-transfected cells (Fig. S5C), although the degree of p53 enhancement varied. However, the induction of p53 by adriamycin treatment was not observed in AIMP2-deficient cells (Fig. 3F) or when AIMP2 was suppressed via siRNA (Fig. S5C), whereas induction of p53 was not affected by the other two treatments, suggesting the specific involvement of AIMP2 in DNA damage-induced cell death.

**Functional Interaction of AIMP2 with p53.** We investigated whether nuclear AIMP2 would interact with p53. Nuclear fractions from UV-irradiated U2OS cells were prepared at different time intervals, and then coimmunoprecipitation of p53 with AIMP2 was performed. The interaction of AIMP2 with p53 increased significantly from 5 to 10 min after UV irradiation (Fig. 4A). The interaction of AIMP2 with p53 was also tested by *in vitro* pull-down assay using GST-p53 and His-AIMP2. His-AIMP2 was coprecipitated with GST-p53 but not with GST alone (Fig. 4B), indicating a direct interaction. The interaction of p53 with AIMP2 was also tested by using a yeast two-hybrid assay. LexA-p53 with B42-AIMP2, but not with B42-AIMP1 (2, 4) and -lysyl-tRNA synthetase (KRS) (14, 21), permitted yeast cell growth on leucine-depleted medium (Fig. 4C), suggesting a specific interaction between p53 and AIMP2. Because AIMP2 is phosphorylated and translocated into the nucleus after UV irradiation, we checked whether phosphorylated AIMP2 had a higher affinity for p53 than unphosphorylated AIMP2. However, both unphosphorylated and phosphorylated AIMP2 bound to p53 with similar affinities (data not shown), suggesting that phosphorylation of AIMP2 does not affect its interaction with p53.

Yeast two-hybrid analyses with B42-AIMP2 and the different fragments of p53 fused to LexA demonstrated that the N-terminal 32 aa of p53 are involved in the interaction with AIMP2 (Fig. 4D). To confirm this conclusion, we tested which p53 mutation (22–24) would affect the interaction with AIMP2. Whereas the p53 mutants at 175 and 248 bound to AIMP2, the mutant at 22/23 lost its binding capability (Fig. 4E), further confirming the interaction of the

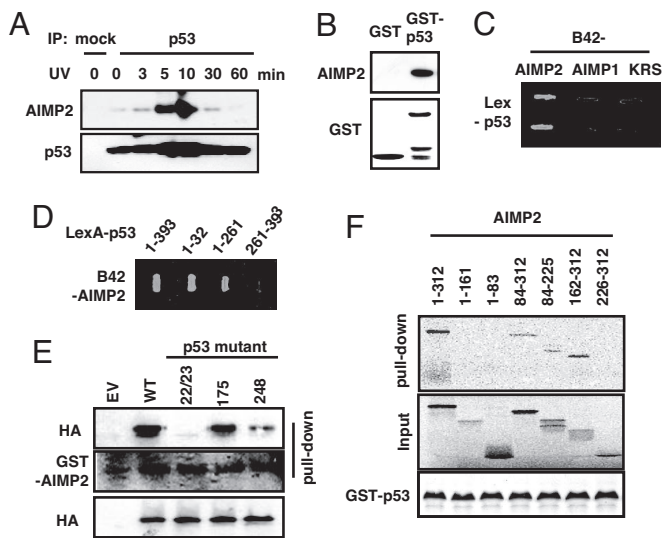


**Fig. 4.** Interaction of AIMP2 with p53. (A) The nuclear fractions were prepared from U2OS cells at the indicated times after UV irradiation and immunoprecipitated with anti-p53 antibody, and the coprecipitation of AIMP2 was determined by Western blotting. (B) p53 was expressed as a GST fusion protein and incubated with recombinant His-tagged AIMP2. GST or GST-p53 proteins were precipitated with glutathione-Sepharose, and the coprecipitation of AIMP2 was determined by Western blotting with an anti-AIMP2 antibody. (C) The interaction of p53 with AIMP2 and two other components of the multi-ARS complex, AIMP1 and KRS, were determined by yeast two-hybrid assay. p53 and the testing partners were expressed as LexA and B42 fusion proteins, respectively, and positive interactions were determined by cell growth on yeast minimal medium. (D) The different peptide regions of p53 were expressed as LexA fusion proteins, and their interactions with B42-AIMP2 were also tested as above. The numbers of each lane indicate the amino acid positions of p53. (E) The WT and different point mutants of p53 at positions 22/23, 175, and 248 (35–37) were radioactively synthesized by *in vitro* translation, mixed with GST-AIMP2, and affinity precipitated with glutathione-Sepharose beads. The p53 mutants coprecipitated with GST-AIMP2 were determined by autoradiography. (F) The radioactively labeled deletion fragments of AIMP2 were prepared by *in vitro* translation, mixed with GST-p53, and precipitated with glutathione-Sepharose beads. The AIMP2 fragments precipitated with GST-p53 were detected by autoradiography. Data are representative of three independent experiments.

N-terminal region of p53 with AIMP2. Conversely, we determined the peptide region of AIMP2 that is involved in its interaction with p53 by *in vitro* pull-down assay. The peptides spanning 84–225, 84–312, and 162–312 aa of AIMP2 interacted with p53 (Fig. 4F), implying that the 162–225 region of AIMP2 was involved in the binding of p53.

To assess the importance of AIMP2 in the activation of p53, we isolated and prepared several AIMP2 mutants and compared their effect during the activation of p53. We identified the I92V, G209S, and E97D/P98L/T99S mutations of AIMP2 from lung cancer cell lines NCI-H157, A549, and NCI-H460, respectively. We also introduced alanine substitutions at E163/N164 and Q172/N173 located in the p53 binding region of AIMP2. We then tested whether any of these mutations would affect the activation of p53 in response to UV irradiation by using a p53-dependent luciferase system. The mutants I92V, E163A/N164A, and Q172A/N173A lost their capability to activate p53 (Fig. S6A). In immunoprecipitation assay, these three mutants (I92V, E163A/N164A, and Q172A/N173A) also showed significantly decreased interactions with p53 (Fig. S6B Upper). Among these mutants, the I92V mutant showed the lowest cellular level when compared with the others (Fig. S6B Lower), suggesting that this mutation might destabilize AIMP2. In fact, the AIMP2 level was lower in NCI-H157 cells in which the I92V mutation was identified (data not shown). The E136A/N164A and Q172A/N173A mutants did not interact with p53 in the pull-down

assay, whereas the I92V mutant retained its ability to interact with p53 (Fig. S6C). We then checked the effects of AIMP2 mutations on the proapoptotic activity of AIMP2. Whereas overexpression of WT AIMP2, the G209S mutant, and the E97D/P98L/T99S mutant enhanced UV-induced cell death, the mutants I92V, E163A/N164A, and Q172A/N173A lost their proapoptotic activity (Fig. S6D). These results demonstrated that p53 activity could be inhibited by mutations in AIMP2, affecting its cellular stability (I92V) or its interaction with p53 (E136A/N164A and Q172A/N173A), further supporting a direct functional linkage between AIMP2 and p53.

**AIMP2 Suppresses MDM2-Mediated Ubiquitination and Degradation of p53.** MDM2 also interacts with the N-terminal region of p53 and this interaction is sensitive to the 22/23 point mutation of p53 (22). Since AIMP2 and MDM2 share the same binding site on p53 (23), we examined whether AIMP2 would compete with MDM2 for the interaction with p53 by coimmunoprecipitation analysis. The binding of MDM2 to p53 was blocked by the presence of AIMP2 (Fig. S7A). In contrast to the full-length AIMP2, the N-terminal 1-83 peptide of AIMP2, which does not interact with p53, did not block MDM2 binding to p53 (Fig. 5A), suggesting that the ability to bind p53 is necessary for the competition with MDM2. We also compared the interaction of p53 and MDM2 in *AIMP2*<sup>+/+</sup> and *AIMP2*<sup>-/-</sup> cells. The binding of MDM2 to p53 was higher in *AIMP2*<sup>-/-</sup> cells than in *AIMP2*<sup>+/+</sup> cells (Fig. S7B). Using *in vitro* binding assays, we checked the competition between AIMP2 and MDM2 for p53 binding. In both directions, the results confirmed their competitive interaction with p53 (Fig. S7C and D). We also tested the relationship of p53 and MDM2 for the interaction with AIMP2. The interaction of p53 with MBP-AIMP2 was decreased by increased amounts of MDM2 (Fig. S7E). Interestingly, AIMP2 also demonstrated weak binding to MDM2 that was suppressed by the addition of p53 (Fig. S7F). To determine whether this interaction has functional meaning or not requires further investigation.

Because MDM2 induces ubiquitin-mediated degradation of p53 (24), AIMP2 is expected to prevent ubiquitination of p53. p53 ubiquitination was suppressed by an increase in AIMP2 (Fig. 5B and Fig. S8A and B), indicating that AIMP2 could block MDM2-mediated ubiquitination of p53. Next, we compared the expression and cellular level of p53 between lung cells isolated from 17.5d *AIMP2*<sup>+/+</sup> and *AIMP2*<sup>-/-</sup> embryos. Although p53 transcription was not affected by the deficiency of AIMP2 as determined by RT-PCR (Fig. S8C Left), its protein level was significantly decreased in *AIMP2*<sup>-/-</sup> cells (Fig. S8C Right), suggesting that AIMP2 enhances the stability of p53. The reduction in p53 was also confirmed by the decreased expression of its targets, *PUMA* and *p21*. We also checked whether p53 stability shows a difference between *AIMP2*<sup>+/+</sup> and *AIMP2*<sup>-/-</sup> MEFs. Proteasome activity was blocked by the treatment with ALLN. After removing ALLN, the decrease in p53 was monitored at different time intervals, whereas protein synthesis was blocked with CHX. The p53 level was more rapidly decreased in *AIMP2*<sup>-/-</sup> cells than in normal cells (Fig. 5C). We checked whether AIMP2 specifically relieves the suppression of p53 activity by MDM2 using a p53-dependent reporter system. The p53 activity was significantly suppressed by the introduction of MDM2 or HDAC3, but only the MDM2-dependent suppression was relieved by the introduction of AIMP2 in a dose-dependent manner (Fig. 5D). Although the UV-dependent increase in p53 levels was not observed in AIMP2-deficient cells, nutlin-3, which inhibits p53-mdm2 interaction (25), recovered the levels of p53 (Fig. 5E). Also, *AIMP2*<sup>-/-</sup> cells became sensitive to UV irradiation when they were treated with nutlin-3 (Fig. S8D), confirming the functional specificity of AIMP2 on p53 action. Taken together, AIMP2 is phosphorylated, dissociated from the multi-ARS complex, translocated into the nucleus, directly interacts with p53, and specifically protects p53 from MDM2-dependent degradation (Fig. 5F).

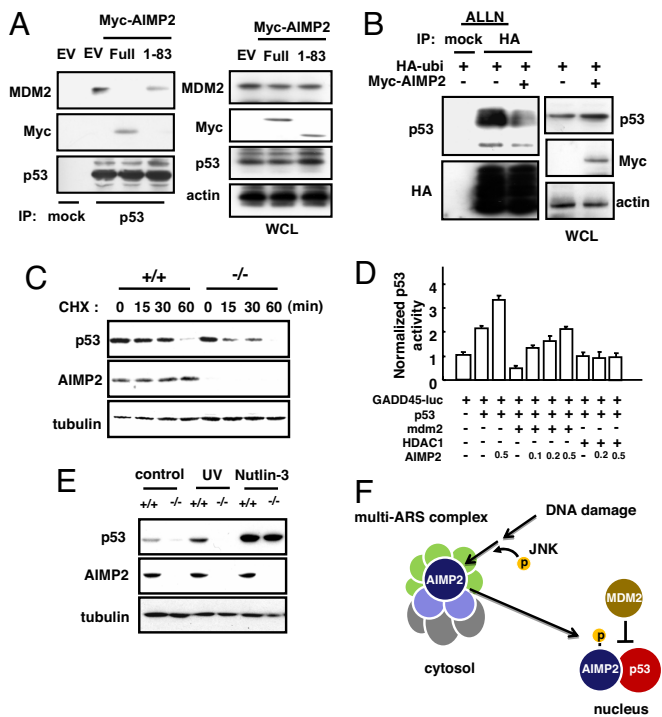


**Fig. 5.** AIMP2 blocks MDM2-mediated ubiquitination and degradation of p53. (A) The full-length and 1 to 83-aa peptide region of AIMP2 were transfected, and their effect on MDM2 binding to p53 was determined by co-immunoprecipitation (Left). Expression of MDM2, Myc-AIMP2 full-length and N-terminal 83-aa fragment, and p53 were determined by Western blotting of whole-cell lysates. Actin was used as a loading control (Right). (B) HA-tagged ubiquitin and Myc-AIMP2 were introduced into U2OS cells, which were then treated with ALLN (20  $\mu$ M) for 3 h. The proteins were extracted and immunoprecipitated with anti-HA antibody, and the precipitated proteins were separated by SDS/PAGE for immunoblotting with an anti-p53 antibody (Upper Left). The ubiquitination of the total precipitated proteins was compared by immunoblotting with an anti-HA antibody (Lower Left). Expression of p53 and AIMP2 was determined by immunoblotting with anti-p53 and -Myc antibodies, respectively (Right). Actin was used as a loading control. (C) U2OS cells were cotransfected with the GADD45-luciferase reporter plasmid (0.2  $\mu$ g) with the indicated amounts of MDM2, HDAC3, and AIMP2. The EV was used to adjust the total amount of DNA, and 0.2  $\mu$ g of pCMV-galactosidase expression vector was used as an internal control. (D)  $AIMP2^{+/+}$  and  $AIMP2^{-/-}$  MEFs were irradiated by UV (50 J/m<sup>2</sup>) or treated with nutlin-3 (5  $\mu$ M) for 6 h. Cells were harvested, and the extracted proteins were subjected to immunoblotting with anti-p53, anti-AIMP2, and anti-tubulin antibodies. (E) Schematic representation of the nuclear translocation of AIMP2 and its interaction with p53 in response to genotoxic stresses. AIMP2 is normally harbored in the multi-ARS complex. Upon DNA damage, AIMP2 is phosphorylated via the JNK pathway, dissociated from the complex, translocated to the nucleus, and bound to p53, which then prevents the MDM2-mediated ubiquitination and degradation of p53.

## Discussion

In this article, we have shown that AIMP2 works as a proapoptotic factor via a direct interaction with p53. Because c-Myc can also activate p53 and enhance p53-dependent apoptosis (26), we were curious to see whether the up-regulation of c-Myc in the absence of AIMP2 (12) would result in the activation of p53. Although levels of FBP and c-Myc in AIMP2-deficient cells are actually higher than in WT cells (12), the level of p53 and its activity are more suppressed, implying that the pathway of AIMP2 to p53 would not be directly linked to the AIMP2-FBP-c-Myc pathway in response to

TGF- $\beta$  or the up-regulation of c-Myc in response to UV irradiation (27).

EPRS was previously shown to be phosphorylated and dissociated from the complex by IFN- $\gamma$  treatment to form a new multi-protein complex that suppresses translation of specific transcripts (28). However, EPRS does not seem to be mobilized by UV irradiation (Fig. 2D), suggesting that the components of the multi-ARS complex respond differentially to incoming stimuli. Despite the importance of AIMP2 for the integrity of the multi-ARS complex (11, 14), the assembly of the whole complex does not seem to be significantly affected by the UV-dependent dissociation of AIMP2. Perhaps the majority of the complex remains intact because the amount of AIMP2 dissociated from the multi-ARS complex upon UV irradiation appears to be minor (Fig. 2A and H). Second, there may be a mechanism to sustain the integrity of the complex through additional modification of other components or refilling the space of AIMP2 with other factor(s) after its dissociation. Third, the disassembly of the complex may occur in a sequential manner rather than simultaneously after the departure of AIMP2. It was not yet determined whether AIMP2 dissociated from multi-ARS complex would exist as a free form or would form another complex with other cellular factors. Considering that EPRS dissociated from the complex by IFN- $\gamma$  forms another multisubunit complex called GAIT, AIMP2 could be recruited to other protein complexes, which may be necessary for the maintenance of cellular stability, nuclear translocation, or the interaction of AIMP2 with p53. Although the interaction of AIMP2 with p53 should be efficient and rapid enough to block the attack of MDM2, AIMP2 should also be able to dissociate from p53 to make way for subsequent processes involving p53. In fact, we observed that AIMP2 showed a decreased affinity toward phosphorylated p53 (data not shown).

Although JNK was shown to be the kinase responsible for the UV-induced phosphorylation of AIMP2, and AIMP2 contains a putative JNK recognition site (data not shown), it is yet to be determined whether JNK is actually the direct upstream kinase of AIMP2. Because the nuclear interaction of AIMP2 with p53 takes place rapidly after UV irradiation, there might be a mechanism involving JNK rapidly responding to UV irradiation that would lead to the activation of AIMP2. Although the early response of AIMP2 involves its posttranslational modification, continuous exposure to genotoxic stresses may accompany the regulation at transcriptional level to refill the depletion of cytosolic portion of AIMP2. Although these questions remain to be solved, the results of this work suggest the existence of tight communication between the cytosolic and nuclear machinery during the maintenance of chromosome integrity and AIMP2 functioning as a unique liaison between them working toward p53 activation during genotoxic stresses. This work also demonstrates that the multi-ARS complex is a molecular reservoir responding to DNA damage, in addition to its role during protein synthesis.

p53 is finely regulated at the transcriptional and posttranscriptional levels (29). Among the diverse pathways leading to p53 activation, AIMP2 appears to specifically respond to DNA damage involving MDM2 but not to regulation by HDAC inhibition or by mitogen treatment (Fig. 3F). Although mitogenic signals such as EGF can also activate p53 via the suppression of MDM2 (20), they may not trigger nuclear localization of AIMP2, unlike the stress induced by DNA damage. Although the regulation mechanisms of p53 have been intensively studied for the last decade (29–31), more regulation mechanisms are expected to be found. Because the balance between p53 and MDM2 is critical for the determination of cell fate, tight feedback regulation of p53 is necessary to prevent the unnecessary hyperactivation of p53 (32). The fine tuning of p53 with a battery of diverse regulators is reflected by the damped oscillations between p53 and MDM2 after DNA damage (33).

It is not clear why AIMP2 has evolved as a modulator of p53. One possibility is that AIMP2 can rapidly respond to genotoxic stresses

because it is ubiquitously present as a component of the translational machinery. In addition, p53 has been known to function as a repressor of RNA polymerase III transcription and inhibits the synthesis of essential small RNAs including tRNAs (34). Therefore, AIMP2 may control tRNA synthesis in coordination with p53 activation, although its role in the regulation of translation requires further investigation. In summary, this work suggests that AIMP2, a scaffolding component of the translational machinery, is a positive and direct regulator of p53 with a unique working mechanism. This work also suggests a potential coordination between cytosolic protein synthesis and nuclear DNA metabolism.

## Materials and Methods

Protocols for well established procedures (cell death, gel filtration chromatography, AIMP2 mutations, immunofluorescence, RT-PCR, binding assays, luciferase assay, two-dimensional electrophoresis, and ubiquitination analysis) can be found in *SI Methods*.

1. Lee SW, Cho BH, Park SG, Kim S (2004) Aminoacyl-tRNA synthetase complexes: Beyond translation. *J Cell Sci* 117:3725–3734.
2. Park SG, Ewalt KL, Kim S (2005) Functional expansion of aminoacyl-tRNA synthetases and their interacting factors: New perspectives on housekeepers. *Trends Biochem Sci* 30:569–574.
3. Park H, et al. (2002) Monocyte cell adhesion induced by a human aminoacyl-tRNA synthetase-associated factor, p43: Identification of the related adhesion molecules and signal pathways. *J Leukoc Biol* 71:223–230.
4. Park SG, et al. (1999) Precursor of proapoptotic cytokine modulates aminoacylation activity of tRNA synthetase. *J Biol Chem* 274:16673–16676.
5. Park SG, et al. (2002) Dose-dependent biphasic activity of tRNA synthetase-associating factor, p43, in angiogenesis. *J Biol Chem* 277:45243–45248.
6. Park SG, et al. (2005) The novel cytokine p43 stimulates dermal fibroblast proliferation and wound repair. *Am J Pathol* 166:387–398.
7. Han JM, Park SG, Lee Y, Kim S (2006) Structural separation of different extracellular activities in aminoacyl-tRNA synthetase-interacting multi-functional protein, p43/AIMP1. *Biochem Biophys Res Commun* 342:113–118.
8. Park SG, et al. (2006) Hormonal activity of AIMP1/p43 for glucose homeostasis. *Proc Natl Acad Sci USA* 103:14913–14918.
9. Park BJ, et al. (2005) The haploinsufficient tumor suppressor p18 up-regulates p53 via interactions with ATM/ATR. *Cell* 120:209–221.
10. Park BJ, et al. (2006) AIMP3 haploinsufficiency disrupts oncogene-induced p53 activation and genomic stability. *Cancer Res* 66:6913–6918.
11. Kim JY, et al. (2002) p38 is essential for the assembly and stability of macromolecular tRNA synthetase complex: Implications for its physiological significance. *Proc Natl Acad Sci USA* 99:7912–7916.
12. Kim MJ, et al. (2003) Down-regulation of FUSE-binding protein and c-myc by tRNA synthetase cofactor p38 is required for lung cell differentiation. *Nat Genet* 34:330–336.
13. Ko HS, et al. (2005) Accumulation of the authentic parkin substrate aminoacyl-tRNA synthetase cofactor, p38/JTV-1, leads to catecholaminergic cell death. *J Neurosci* 25:7968–7978.
14. Han JM, et al. (2006) Hierarchical network between the components of the multi-tRNA synthetase complex: Implications for complex formation. *J Biol Chem* 281:38663–38667.
15. Keller DM, et al. (2001) A DNA damage-induced p53 serine 392 kinase complex contains CK2, hSpt16, and SSRP1. *Mol Cell* 7:283–292.
16. Matsui MS, DeLeo VA (1990) Induction of protein kinase C activity by ultraviolet radiation. *Carcinogenesis* 11:229–234.
17. Sabapathy K, et al. (2004) Distinct roles for JNK1 and JNK2 in regulating JNK activity and c-Jun-dependent cell proliferation. *Mol Cell* 15:713–725.
18. Roy S, Packman K, Jeffrey R, Tenniswood M (2005) Histone deacetylase inhibitors differentially stabilize acetylated p53 and induce cell cycle arrest or apoptosis in prostate cancer cells. *Cell Death Differ* 12:482–491.
19. Yoshida M, Kijima M, Akita M, Beppu T (1990) Potent and specific inhibition of mammalian histone deacetylase both in vivo and in vitro by trichostatin A. *J Biol Chem* 265:17174–17179.
20. Sherr CJ, Weber JD (2000) The ARF/p53 pathway. *Curr Opin Genet Dev* 10:94–99.
21. Park SG, et al. (2005) Human lysyl-tRNA synthetase is secreted to trigger proinflammatory response. *Proc Natl Acad Sci USA* 102:6356–6361.
22. Asher G, Lotem J, Sachs L, Kahana C, Shaul Y (2002) Mdm-2 and ubiquitin-independent p53 proteasomal degradation regulated by NQO1. *Proc Natl Acad Sci USA* 99:13125–13130.
23. Sherr CJ (2001) The INK4a/ARF network in tumour suppression. *Nat Rev Mol Cell Biol* 2:731–737.
24. Yang Y, Li CC, Weissman AM (2004) Regulating the p53 system through ubiquitination. *Oncogene* 23:2096–2106.
25. Vassilev LT, et al. (2004) In vivo activation of the p53 pathway by small-molecule antagonists of MDM2. *Science* 303:844–848.
26. Eischen CM, Weber JD, Roussel MF, Sherr CJ, Cleveland JL (1999) Disruption of the ARF-Mdm2-p53 tumor suppressor pathway in Myc-induced lymphomagenesis. *Genes Dev* 13:2658–2669.
27. Blattner C, et al. (2000) UV-Induced stabilization of c-fos and other short-lived mRNAs. *Mol Cell Biol* 20:3616–3625.
28. Sampath P, et al. (2004) Noncanonical function of glutamyl-prolyl-tRNA synthetase: Gene-specific silencing of translation. *Cell* 119:195–208.
29. Toledo F, Wahl GM (2006) Regulating the p53 pathway: In vitro hypotheses, in vivo veritas. *Nat Rev Cancer* 6:909–923.
30. Levine AJ, Finlay CA, Hinds PW (2004) P53 is a tumor suppressor gene. *Cell* 116:567–69.
31. Levine AJ (1997) p53, the cellular gatekeeper for growth and division. *Cell* 88:323–331.
32. Ma L, et al. (2005) A plausible model for the digital response of p53 to DNA damage. *Proc Natl Acad Sci USA* 102:14266–14271.
33. Lahav G, et al. (2004) Dynamics of the p53-Mdm2 feedback loop in individual cells. *Nat Genet* 36:147–150.
34. Cairns CA, White RJ (1998) p53 is a general repressor of RNA polymerase III transcription. *EMBO J* 17:3112–3123.
35. Baker SJ, et al. (1989) Chromosome 17 deletions and p53 gene mutations in colorectal carcinomas. *Science* 244:217–221.
36. Lin J, Chen J, Elenbaas B, Levine AJ (1994) Several hydrophobic amino acids in the p53 amino-terminal domain are required for transcriptional activation, binding to mdm-2 and the adenovirus 5 E1B 55-kD protein. *Genes Dev* 8:1235–1246.
37. Powell B, Soong R, Iacopetta B, Seshadri R, Smith DR (2000) Prognostic significance of mutations to different structural and functional regions of the p53 gene in breast cancer. *Clin Cancer Res* 6:443–451.

**Cell Culture and Reagents.** Cell lines were obtained from American Type Culture Collection and maintained in 10% FBS containing McCoy's 5a for U2OS cells. MEFs were obtained from 12.5-d embryos as described (9, 12). Polyclonal rabbit antibodies against p53 (FL-393) and MDM2 (C-18) were purchased from Santa Cruz Biotechnology, adriamycin, trichostatin A (TSA), and nutlin-3 from Sigma, and ALLN, CHX, staurosporin, JNK inhibitor II, CK2 inhibitor, U0126, SB202190, and EGF from Calbiochem. The anti-AIMP2 antibody was described above (11).

**Exogenous Expression.** We transfected DNA using the geneporter system (Gene Therapy System). The expression vectors of WT and mutant p53, as well as MDM2, were kindly provided by Dr. T. H. Han (Sungkyunkwan University, Seoul, Korea), Dr. H. W. Lee (Yonsei University, Seoul, Korea), and Dr. H. D. Youn (Seoul National University, Seoul, Korea), respectively. The siRNA against AIMP2 and control siRNA with a random sequence were obtained from Invitrogen (14).

**ACKNOWLEDGMENTS.** This work was supported by Korea Science and Engineering Foundation (KOSEF) Grants R17-2007-020-01000-0 and M10534040002-07N3404-00210, funded by the Korean Government (MOST).